Interference-aware Co-channel Transmission over DTV Bands via Partial Frequency and Time Overlaps

Anshul Thakur[a,b], Swades De[b], and Gabriel-Miro Muntean[c]
[a]Centre for Development of Telematics, New Delhi, India
[b]Department of Electrical Engineering and Bharti School of Telecommunication, IIT Delhi, New Delhi, India
[c]Performance Engineering Laboratory, School of Electronic Engineering, Dublin City University, Ireland

***Abstract*— This paper studies coexistence scenario of deploying secondary communication networks in a co-channel mode within TV bands where a primary broadcaster is present. Keeping in view the differences in timing and spectral characteristics between the primary and secondary transmission systems, subcarrier-level interference at the primary is computed in presence of time-and-frequency overlapped secondary transmission. This estimation is validated experimentally as well as via simulations. Specifically, the possibility of coexistent secondary transmission near the primary broadcast receivers is experimentally evaluated in an emulated digital video broadcast - terrestrial second generation (DVB-T2) transmission environment. The analytical results and the experimental studies demonstrate that the effects of interference at the primary receiver are within tolerable range even when the secondary transmitter transmits at high power with appropriately chosen time-frequency occupancy overlaps. The benefits are further enhanced when the agility of frequency and temporal overlaps are combined with power control in the secondary network.**

I. Introduction

Spectrum regulatory agencies worldwide have been opening up the television (TV) broadcast radio spectrum for cognitive access for better utilization [1], [2]. Following these relaxations, a number of standards, such as, Long-Term Evolution - unlicensed (LTE-U), IEEE 802.22 wireless regional access network (WRAN), and IEEE 802.11af have sprung up or expanded in scope to encompass the new spectrum and its usage possibilities. Owing to its excellent propagation characteristics, the higher end of the Digital Terrestrial TV (DTV) band has been reallocated for cellular communication deployments in many telecommunication regions of the world. Further, International Telecommunication Union - Radio (ITU-R) has emplaced the discussion on deciding about the rest of the DTV band for 2023 and has invited more comprehensive studies exploring the new radio band access paradigm [3].

However, despite the relaxation, current regulations forbid any secondary network deployment within a demarcated coverage region of a primary broadcast network to allay possibilities of broadcast (primary) service quality degradation through interference. It has been argued in [4] that the current regulations on cognitive radios take a very transmit-centric view of the situation while completely ignoring the receiver side issues, particularly in the terrestrial broadcast bands.

Coexistence between DTV and any other heterogeneous solutions has been studied through limited test-beds and experiments [5], [6]. Further, the existing studies have solely focused on standardized technologies in their current forms. To this end, similar to LTE-U and 802.11af technologies that are targeted to adaptively coexist, we argue that modification in upcoming cognitive access technologies will likely enable a better coexisting communication ecosystem with the DTV broadcast technology as well. We also note that, previous studies on coexistent secondary transmission and DTV broadcast have focused on variable spectral overlap only.

To complement the prior studies on coexistent secondary communication in the DTV bands, in this work, we study the effect of co-channel interference from secondary transmission on the primary OFDM system in a general way with few simple assumptions. An expression for interference to the primary receiver experienced at the subcarrier level is obtained. The interference estimate is then compared with the simulation-based results as well as experimental studies in two main secondary interference scenarios: variable frequency overlap, and variable temporal occupancy. The effects of varying the subcarrier density are then explored. In some cases, the above two scenarios are also combined with power controlled secondary transmission. To the best of our knowledge, no other works have studied more than the frequency overlap aspects of these coexistence scenarios.

The contributions of this paper are two-fold: (1) It presents a general framework for analyzing co-channel interference. (2) It demonstrates the possibility of achieving coexistence between the primary broadcast network and secondary communication network by combining flexibilities over multiple dimensions in the secondary network, namely, power control, link-scheduling, and spectral occupancy in DTV spectrum bands. We believe that this ground work will make useful space towards further investigations on quality of service guarantee of coexisting unlicensed secondary communications in the active DTV bands.

The paper is organized as follows. In the next section, we briefly survey the related works. In Section III we present the system model and enumerate the main assumptions. The experimental methodology is described in Section IV, and the performance results are presented and discussed in Section V. Finally, concluding remarks are drawn in Section VI.

II. Related Works

Several researchers have conducted recent studies on the possibility of coexistence between a digital broadcast over primary network and another orthogonal frequency division multiplexing (OFDM)-based secondary communication network, namely LTE [7] and IEEE 802.22 WRAN [8]. Coexistence of TV broadcast technologies like Digital Video Broadcast-Terrestrial (DVB-T) and its second generation DVB-T2 with IEEE 802.22 and other OFDM based systems have been studied in laboratory environments [5], [6]. Most of these works are based on experimental test-beds or numerical simulations where the interference of one system on the other was studied to determine the acceptable level of interference in the form of Carrier-to-Interference (C/I) ratio, for various transmission parameters of the primary system. Some operating configurations in which an interferer may impact the primary broadcast reception, or in some converse cases where DTV acts as an interferer, have been reported in [8], [5], [6]. C/I protection ratios required for LTE-A femto-cell operation indoors while having varying degree of channel overlaps with the primary DTV broadcast were evaluated in [9]. These studies indicate that for small overlaps between frequency bands of the primary and secondary networks, the impact of interference is small. The operating configurations in which an LTE system may be deployed depending on the amount of spectral overlap were experimentally evaluated in [10]. The coexistence scenario between DVB-T2 and LTE was studied in [11], where the authors made keen observations about the difference in signal structures of the two schemes while analytically deriving average ergodic capacities of the systems aiming at spectral overlap optimization. However, all of these studies have focused on the coexistence of existing technologies deployed as-is, without regard to the key differences in signal structures, framing, and link-scheduling of the two heterogeneous technologies.

Effects of narrow-band interferers on OFDM reception by modeling the post-DFT (digital Fourier transform) effects of interference on each subcarrier symbol detection and methods of mitigating these effects were studied in [12], [13]. However, the extent of degradation in service was not analyzed in these works. The effect of narrow-band interference on the primary OFDM signal using the power spectral density (PSD) of the signals involved was done in [14], [15]. Taking the frequency spectrum of an OFDM subcarrier as a $sinc$ function, these studies estimated the effect of one or a few narrow-band interference sources on the OFDM signal using relative interference power as measurement metric.

Studies analyzing co-channel interference among OFDM-based systems have mostly catered to homogeneous deployment scenarios like cellular deployments where the interferer is a cell operating with the same parameters. The effect of carrier frequency offsets on OFDM performance was studied in [16], [17], [18]. Other co-channel interference due to self-generated artifacts have mostly been mapped on to changes in carrier frequency offsets and were studied from that perspective. The study in [19] showed that the estimates from the above approach and the PSD based approach are overestimates as they do not consider misalignment between the coexisting parties.

III. System Model

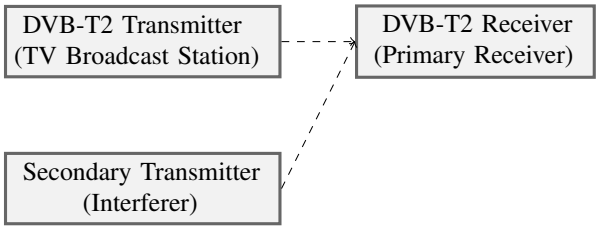

Fig. 1. Interference scenario.

We consider a primary DVB-T2 broadcast system operating with N-point FFT and a symbol duration of T_s^p. A secondary LTE-like system with M-point FFT ($M \ll N$) and symbol duration T_s^s ($T_s^s \ll T_s^p$) is operating in co-channel mode with the primary network as represented in 1. The assumption T_s^s
llT_s^p represents the typical working configurations in existing technologies. For example, DVB-T2 has a symbol duration of 448 μs while LTE symbol is of 66.7 μs. The signal received at the primary receiver can be written as:

$$r(t) = s_p(t) + \sum_{i=0}^{L} s_{s,i}(t - iT_s^s) + \mathbf{n}(t). \tag{1}$$

The first term in the equation (1) represents the signal received at the primary (broadcast) receiver from the broadcast transmitter; the second term is the interference component received due to secondary transmission. L is the Number of interfering symbols received given by (T_s^p/T_s^s). For simplicity of analysis, it is assumed that $L \in \mathbb{Z}$. In the analysis, we assume time synchronization between the first OFDM symbol of the primary signal and the first OFDM symbol of the secondary signal.

Sampling the signal $r(t)$ with a sampling period of $T = N/T_s^p$, the nth sample of the received signal may be expressed as:

$$\begin{aligned} r[n] =& s_p(nT) + \sum_{i=0}^{L-1} s_{s,i}(nT - iT_s^s) + \mathbf{n}[nT] \\ =& \sum_{k=0}^{N-1} a_k D_k e^{j2\pi \frac{k}{T_s^p} nT} \\ &+ \sum_{i=0}^{L-1} \sum_{m=0}^{M-1} q b_m C_m^{(i)} e^{j2\pi \frac{m}{T_s^s}(nT - iT_s^s)} + \mathbf{n}[nT]. \end{aligned} \tag{2}$$

Here, a_k and b_m are the channel gains for the kth and mth subcarriers of primary and secondary systems respectively, assuming that the gains do not change for the entire primary symbol duration. D_k is the data symbol transmitted by the

primary on its kth subcarrier. $C_m^{(i)}$ is the data carried in the mth subcarrier of the ith overlapping secondary symbol. q is an interpolation factor incurred at the primary receiver due to improper sampling of the secondary signal by an amount NT_s^s/MT_s^p. For most operating conditions, $NT_s^s/MT_s^p > 1$ holds. We assume q to be 1 for simplicity of analysis. In simulations, we use $sinc$ interpolation for secondary signal reconstruction which takes care of the general case.

The symbol value at the lth primary subcarrier after the DFT operation can be written as:

$$\begin{aligned} R_l &= \sum_{n=0}^{N-1} r[n] e^{-j2\pi \frac{nl}{N}} \qquad (3)\\ &= \sum_{n=0}^{N-1} \Bigg\{ \sum_{k=0}^{N-1} a_k D_k e^{j2\pi \frac{nk}{N}} \\ &\quad + \sum_{i=0}^{L-1} \sum_{m=0}^{M-1} b_m C_m^{(i)} e^{j2\pi \frac{mn}{N} \frac{T_s^p}{T_s^s}(1-\frac{i}{n}\frac{T_s^s N}{T_s^p})} + \mathbf{N}[n] \Bigg\} e^{-j2\pi \frac{nl}{N}} \\ &= \sum_{n=0}^{N-1} \sum_{k=0}^{N-1} a_k D_k e^{j2\pi \frac{n}{N}(k-l)} \\ &\quad + \sum_{n=0}^{N-1} \sum_{i=0}^{L-1} \sum_{m=0}^{M-1} q b_m C_m^{(i)} e^{j2\pi \frac{n}{N}[\frac{mT_s^p}{T_s^s} - \frac{miN}{n} - l]} + \mathbf{N}[l]. \end{aligned}$$

$$\text{or, } R_l = \frac{a_l D_l}{N} + I_l \qquad (4)$$

where, the interference term I_l can be written as:

$$\begin{aligned} I_l &= \sum_{n=0}^{N-1} \sum_{i=0}^{L-1} \sum_{m=0}^{M-1} q b_m C_m^{(i)} e^{j2\pi \frac{n}{N}[\frac{mT_s^p}{T_s^s} - \frac{miN}{n} - l]} \\ &= \sum_{n=0}^{N-1} \sum_{i=0}^{L-1} \sum_{m=0}^{M-1} q b_m C_m^{(i)} e^{j2\pi \frac{n}{N}[\frac{mT_s^p}{T_s^s} - l]} e^{-j2\pi mi} \\ &= \sum_{i=0}^{L-1} \sum_{m=0}^{M-1} q b_m C_m^{(i)} e^{-j2\pi mi} \sum_{n=0}^{N-1} e^{j2\pi \frac{n}{N}[mL-l]} \qquad (5) \end{aligned}$$

By geometric sum, the expression in (5) simplifies to:

$$I_l = \sum_{i=0}^{L-1} \sum_{m=0}^{M-1} K b_m C_m^i e^{-j2\pi mi} e^{j\pi(1-\frac{1}{N})(Lm-l)} \mathcal{A}, \qquad (6)$$

where $\mathcal{A} = \left[\frac{sinc\left([Lm-l]\right)}{sinc\left(\frac{1}{N}[Lm-l]\right)} \right]$ and K is a scaling constant. The effect of varying the number of time slots the secondary system is transmitting, i ($i \leq L$) and varying the number of primary subcarriers which are interfered by the secondary by varying M for a fixed T_s^s can now be studied. By varying T_s^s for a fixed bandwidth, or varying the bandwidth and T_s^s for a fixed number of subcarriers can also be studied using the same equation. The number of primary subcarriers interfered by the secondary can be written as:

$$\eta = \left\lceil \frac{MT_s^p}{T_s^s} \right\rceil \qquad (7)$$

In this work, we are interested in the average signal-to-noise-and-interference ratio (SINR) at the primary receiver across all the subcarriers. Assuming uniform power allocation across all subcarriers, SINR can be written as:

$$\text{SINR} = \frac{1}{N} \sum_{l=0}^{N-1} \frac{|\, a_l D_l \,|^2}{|\, I_l \,|^2 + N_o} \qquad (8)$$

where I_k is given by (6) and N_o is the noise power. The equation (8) takes into account the effects of having multiple secondary symbols through parameter L and the amount of spectral overlap by the relation between bandwidth and number of subcarriers for a fixed symbol duration given in (7). In this formulation, subcarrier density in the secondary system can be varied according to the chosen value of T_s^s. Effects of these variations have been studied experimentally and are presented in the next section.

IV. Experimental Setup

A. Primary DTV Broadcast Network

DVB-T2 is used as the primary broadcast system with parameters enumerated in Table I. The transmitter chain is implemented in GNU-Radio. The DTV receiver used is an inexpensive commercial off-the shelf DTV receiver. This ensures that the observations are as close to a typical deployment scenario. The reception is studied for the case when the primary receiver has good reception of the primary signal, i.e., has a good signal-to-noise ratio (SNR) at the receiver in the absence of any interference.

TABLE I
PRIMARY (DVB-T2) PARAMETERS

Center Frequency	429 MHz
Bandwidth	7.6094 MHz (8 MHz)
FFT Size	4096
Active Subcarriers	3409
Guard Interval	1/32
Code Rate	2/3
Modulation	64 QAM
Symbol Duration	448 μs

B. Secondary Network

The secondary transmitter uses an LTE-like OFDM transmitter chain implemented in GNU Radio. The parameters used are listed in Table II.

TABLE II
SECONDARY TRANSMITTER PARAMETERS

Bandwidth	4.703 MHz (5 MHz)
FFT-Size	512
Active Subcarriers	301
Guard Interval	1/32
Modulation	QPSK
Symbol Duration	64 μs

The secondary transmitter is designed to have a gated transmission scheme where the duration for which it transmits can be controlled in multiples of one time slot duration. The transmit power and center frequency of the transmission can also be controlled. Being an opportunistic network, it is assumed that the secondary system is fully capable of operating in the presence of a strong primary signal by employing appropriate interference cancellation techniques and knowledge of the primary signal's structure.

C. Methodology

For all the experimental variations, the setup was unchanged physically to ensure minimal deviation due to setup errors. The primary transmitter's transmit power was set so as to receive a good SINR value of 20 dB at a test receiver placed at a fixed distance from the transmitter. A continuous MPEG transport stream was used as payload. It was verified that reception at the receiver was error-free.

The SDR acting as secondary transmitter was first calibrated to obtain tables for different transmit power levels and the appropriate settings in the device and GNU Radio. The maximum transmit power of the secondary transmitter and its distance from the primary receiver was set so that the SINR observed at a secondary receiver co-located with the primary receiver was equal to the SINR received by the primary receiver (20 dB) when only one of the networks is operational. A random bit stream was used as payload.

The secondary system transmitted was set to transmit in all slots in the adjacent band initially. Then, with small increments of 16 subcarriers (0.25 MHz width) at a time, its band was shifted into the primary's band, increasing the amount of spectral overlap. For each iteration, the SINR at the primary receiver was observed.

The same procedure was then repeated for different number of time slots varying from full occupancy at 7 time slots to minimal occupancy at 1 time slot. Finally, the entire procedure was repeated for lower transmit power levels of the secondary transmitter.

To explore the effects of varying the subcarrier density, bandwidth (B) was held constant at 5 MHz. The number of active subcarriers (M) was chosen iteratively from $[64, 128, 256, 512]$. Then, for complete spectral overlap, the performance of each setting was observed and compared with the analytical results.

V. Results and Discussions

Figure 2 shows the variation of C/I ratios for varying spectral overlap. As observed in [5], [7], and [20] as well, this C/I must be maintained at the primary receiver to ensure proper reception. In agreement to the observations in [7] where coexistence of LTE based secondary system was studied, there is a sharp decline in the required C/I ratios at 20% spectral overlap. Thus, the maximum amount of power that a secondary transmitter is allowed to use is restricted by these protection ratios. But since these are the conditions prevailing at the primary receiver, the amount of power that the secondary can transmit and the amount of interference that is caused by it depends on the knowledge of the operating conditions of the primary receiver.

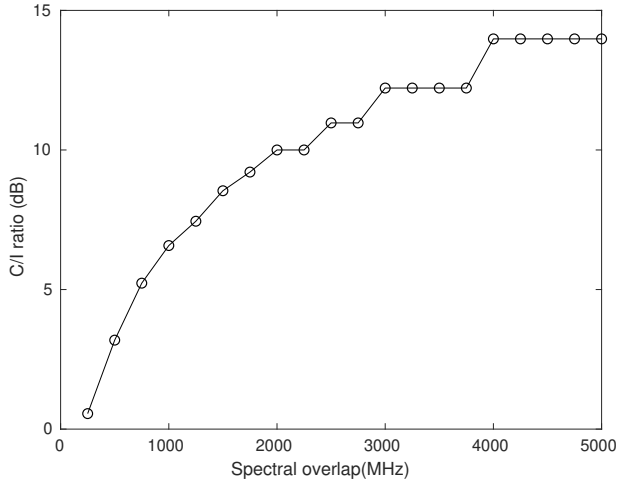

Fig. 2. Carrier to interference protection ratios for varying spectral overlap.

A. Variable Frequency Overlap

For a fixed secondary transmit power and full time occupancy, performance degradation of the primary system due to varying spectral overlap is shown for two secondary power levels in Figure 3. For proper reception, an SINR of at least 14 dB was required at the primary receiver. It is seen that the SINR dips below the threshold for an overlap over 1 MHz. On reducing the secondary power, more and more spectral overlap becomes acceptable while sustaining good reception.

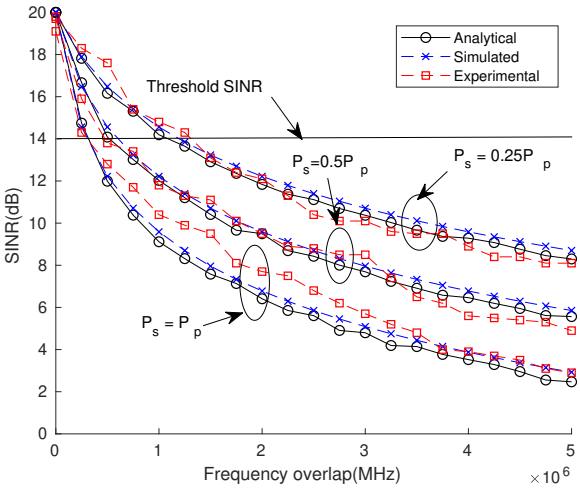

Fig. 3. SINR variation of primary with varying spectral overlap.

B. Variable Temporal Occupancy

For fixed secondary transmit power and spectral overlap held at 5 MHz, performance degradation of the primary system for variable time occupancy is shown in Figure

4. Compared to variable spectral overlap, the degradation is more pronounced in this case for each increase in slot occupancy. It can be seen in equation (6), each slot adds its own complete contribution to interference which outweighs a similar fractional increase in spectral overlap. Thus, greater the number of time slots for which secondary signal is present, worse the performance of the primary system due to accumulation of power. This observation from the expression (6) must hold even for the case when number of available time slots varies due to choice of a different subcarrier density. This is indeed the case and is validated ahead. For an SINR threshold of 14 dB, neither pure spectral overlap nor pure temporal overlap yield sustainable secondary networks for most variations. However, temporal occupancy and spectral overlap being independent dimensions, a mixed mode of operation that employs both time and frequency aspects would give a performance better than when using both independently.

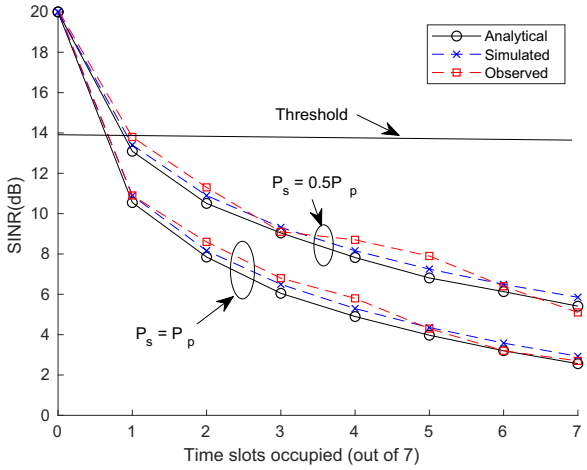

Fig. 4. SINR variation of primary with varying time occupancy.

C. Variable Subcarrier Density

For a fixed spectral overlap of 5 MHz and full power of the secondary (interfering) transmitter, the performance of the primary system with varying the interfering transmission's subcarrier density and number of time slots in each case was observed. For a comparative evaluation between the systems, the time occupancy is expressed in terms of fraction of primary symbol time in Figure 5. It is observed that when all subcarriers are in active use (which is not the case practically) then, for the same time occupancy, various subcarrier densities incur comparable performance degradation in primary reception. This can be used in choosing the symbol timing and an appropriate framing structure of the secondary network given a data rate constraint.

D. Discussions

In the current digital broadcast regime, the receivers only listen and do not transmit anything back to the transmitter. This arrangement allows the primary transmitter to maximize

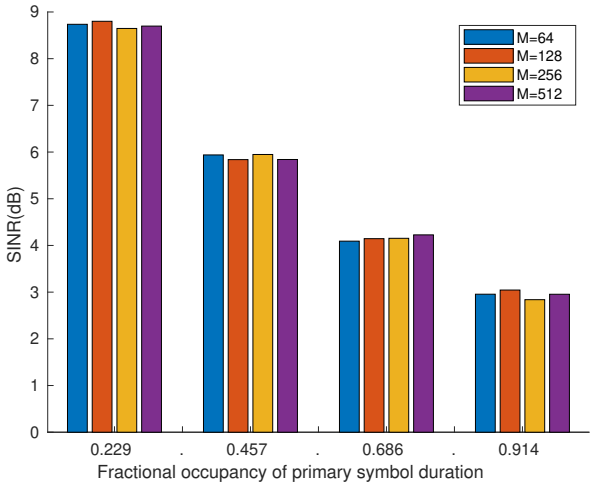

Fig. 5. SINR variation with varying time occupancy and subcarrier density.

coverage radius by employing large power. In contrast to this, the secondary networks envisioned in this work are aimed at bidirectional communication and the inter-node distance is at least an order smaller than the primary DTV broadcast network. Hence, power requirements are lesser are also lesser than that of the primary system.

If the conditions prevailing at the primary receivers in the region between the communicating secondary nodes can be known through some means - querying an extensive geolocation database for example - the secondary system can adapt its own parameters in time, frequency and power to achieve certain rate guarantees. In the regions that receive abundant to over-abundant signal from the primary transmitter, the amount of transmit power at the disposal of the secondary transmitter to maintain the same C/I ratio is expected to be high. These regions are usually to be found deep inside the protection contour near to the transmitter. Thus, such secondary transmitters in these regions can work with higher power levels and hence, provide better data rates or operate over longer distances. As the received signal quality for the primary receiver deteriorates, the margin in power, time, and frequency decreases and the secondary devices must make various trade-offs while trying to maximize the data rate. This would have impact on the deployment density of secondary nodes in the region. Thus, the operating parameters of the secondary system are intimately tied with the signal quality being received at the primary receiver. The expressions obtained in this work can then be used to find out the best set of parameters among power, time slots and spectral occupancy of the secondary system.

Some simple devices may not have power control mechanisms in them. For these devices, a minimum power level must be maintained. In such cases, an optimal selection of temporal occupancy, spectral overlap and subcarrier density may be chosen to ensure sustainable communication. As an example, Table III highlights in bold the operating settings that maximize secondary data rate for various configurations

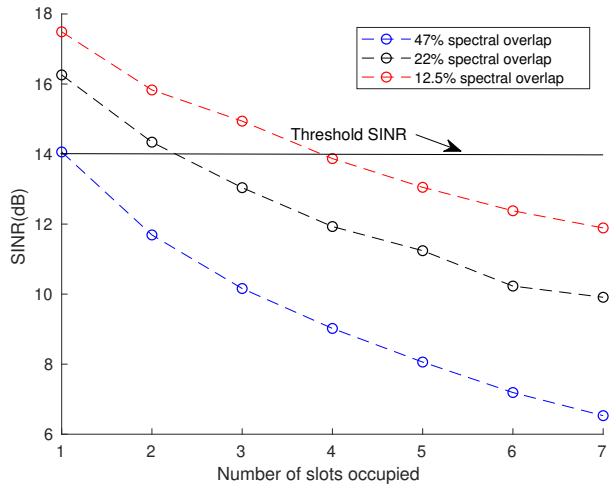

Fig. 6. SINR variation with varying time occupancy and spectral overlap.

when received secondary power P_s is half of received primary power P_p and the tolerance threshold set for primary reception is 14.0 dB. QPSK modulation is used in this example. Further, Figure 6 indicates that the secondary transmitter may be able to use higher transmit power and a greater spectral overlaps by reducing its temporal occupancy. Thus, in comparison to [7], the combination of temporal and spectral overlap offers better performance for the secondary network while maintaining good reception at the primary receiver.

TABLE III

SINR COMPARISON: BANDWIDTH VERSUS TIME SLOTS (P_s = 0.5 P_p)

Time slots / BW (MHz)	1	2	3	4	5	6	7
0.25	19.22	18.72	18.22	17.33	17.38	16.38	16.52
0.50	18.57	17.46	16.63	15.82	**15.03**	**14.94**	**14.09**
0.75	17.99	16.55	15.74	**14.83**	13.92	13.55	12.95
1.00	17.49	15.83	**14.94**	13.87	13.05	12.38	11.89
1.25	17.04	15.43	13.99	13.06	12.47	11.56	11.19
1.50	16.63	14.71	13.46	12.31	11.64	10.98	10.38
1.75	16.26	**14.34**	13.04	11.93	11.24	10.23	9.91
2.00	15.91	13.84	12.46	11.49	10.79	9.92	9.21
2.25	15.59	13.39	11.99	10.95	10.16	9.35	8.83
2.50	15.29	13.31	11.52	10.41	9.54	8.85	8.29
2.75	15.02	12.84	11.23	10.21	9.43	8.50	7.89
3.00	14.76	12.49	11.02	9.95	8.93	8.45	7.63
3.25	14.51	12.09	10.73	9.52	8.54	8.05	7.35
3.50	14.28	11.82	10.34	9.17	8.38	7.44	6.93
3.75	**14.06**	11.69	10.16	9.02	8.06	7.19	6.53
4.00	13.85	11.31	9.74	8.78	7.71	7.07	6.39
4.25	13.64	11.19	9.84	8.41	7.59	6.89	6.18
4.50	13.45	11.12	9.53	8.14	7.45	6.52	5.89
4.75	13.27	10.76	9.03	7.82	7.23	6.24	5.62
5.00	13.09	10.52	8.94	7.72	6.93	6.13	5.39
Maximum rate supported (Mbps)							
	1.07	1.0	0.86	0.86	0.72	0.86	1.0

A smaller symbol duration allows packing more symbols in a given time and hence allowing smaller frame sizes while maintaining the same raw data rate. The higher layer protocols can better take care of retransmission of data carried in a few lost symbols out of many, rather than in the case when the same amount of data is carried in fewer symbols packed within the same duration. Further, when data rate requirements are small, for example in case of low power wireless sensor networks, a smaller symbol time and channel occupancy duration can be selected to enable communication without affecting the primary reception. As an example, for a data rate requirement of 1 Mbps, transmit power fixed at $0.5P_p$ and full spectral overlap of 5 MHz, various configurations supporting this data rate using QPSK are highlighted in Table IV. It is observed that FFT-sizes of 256 and 512 do not support co-channel operation at all. However, for 50% spectral overlap with other requirements being the same, even FFT-size of 256 allows co-channel operation. This is highlighted in Table V

TABLE IV

SINR COMPARISON: BANDWIDTH VERSUS TIME SLOTS (P_s = 0.5 P_p, FULL SPECTRAL OVERLAP)

N-FFT / Time slots	64	128	256	512
1	**17.5**	**15.91**	13.86	11.4
2	**15.92**	13.79	11.38	8.64
3	**14.71**	12.54	9.98	7.06
4	13.85	11.52	8.59	5.89
5	13.04	10.72	7.65	
Maximum rate supported (Mbps)				
	8.5	5.9	0	0

TABLE V

SINR COMPARISON: FFT SIZE (N) VERSUS TIME SLOTS (P_s = 0.5 P_p, 50% SPECTRAL OVERLAP)

N-FFT / Time slots	64	128	256	512
1	**18.57**	**17.5**	**15.91**	13.84
2	**17.44**	**16.12**	**14.06**	11.36
3	**16.79**	**14.72**	12.53	9.82
4	**15.73**	13.91	11.34	8.68
5	**15.16**	13.03	10.49	0
6	**14.93**	12.44	10.20	0
Maximum rate supported (Mbps)				
	10	8.8	12.5	0

Thus, by an optimal selection of parameters, the data rate in the secondary network can be maximized while ensuring insignificant degradation on primary reception.

VI. CONCLUDING REMARKS

In this work, we have studied analytically and experimentally the performance of primary DTV broadcast system in the presence of an OFDM-based secondary (interfering) network. Dimensions of variable power, time, and frequency

have been explored to find how the signal differences between the two heterogeneous systems may be exploited by the secondary system to achieve coexistent secondary transmission within the interference limit of the primary reception system. From our experimental observations, supported by analytical estimates, we have proposed a secondary transmission scheme which enables selection of the optimum transmission parameters that would enable coexistent presence of secondary users in the DTV broadcast signal reception regions.

As a future extension of this work, we intend to quantify the achievable secondary quality of service and quality of user experience under various primary signal strength scenarios, as well as the required optimum secondary transmitter parameter selection to enable achieving predefined user service/experience guarantees of these coexistent systems.

REFERENCES

[1] FCC, "In the Matter of Unlicensed Operation in the TV Broadcast Bands (ET Docket No. 04-186), Additional Spectrum for Unlicensed Devices Below 900 MHZ and in the 3 GHz Band (ET Docket No. 02-380), Second Report and Order and Memorandum Opinion and Order," Federal Communications Commission (FCC), Technical Report (TR), 11 2008. [Online]. Available: https://hraunfoss.fcc.gov/edocs_public/attachmatch/FCC-08-260A1.pdf

[2] Ofcom, "Digital dividend - cognitive access Statement on licence-exempting cognitive devices using interleaved spectrum," The Office of Communications (Ofcom), Technical Report (TR), 07 2009.

[3] ITU, "Final Acts WRC-15, World Radiocommunication Conference (Geneva, 2015)," ITU, Tech. Rep. (TR), 2015. [Online]. Available: https://www.itu.int/dms_pub/itu-r/opb/act/R-ACT-WRC.12-2015-PDF-E.pdf

[4] R. Ramjee, S. Roy, and K. Chintalapudi, "A critique of FCC's TV white space regulations," *GetMobile: Mobile Comp. and Comm.*, vol. 20, no. 1, pp. 20–25, Jul. 2016.

[5] V. Popescu, M. Fadda, M. Murroni, J. Morgade, and P. Angueira, "Co-channel and adjacent channel interference and protection issues for DVB-T2 and IEEE 802.22 WRAN operation," *IEEE Trans. Broadcast.*, vol. 60, no. 4, pp. 693–700, Dec. 2014.

[6] V. Popescu, M. Fadda, and M. Murroni, "Performance analysis of IEEE 802.22 wireless regional area network in the presence of digital video broadcasting - second generation terrestrial broadcasting services," *IET Commun.*, vol. 10, no. 8, pp. 922–928, 2016.

[7] J. Ribadeneira-Ramírez, G. Martínez, D. Gómez-Barquero, and N. Cardona, "Interference analysis between digital terrestrial television (DTT) and 4G LTE mobile networks in the digital dividend bands," *IEEE Trans. Broadcast.*, vol. 62, no. 1, pp. 24–34, Mar. 2016.

[8] V. Popescu, M. Fadda, M. Murroni, and D. Giusto, "Coexistence issues for IEEE 802.22 WRAN and DVB-T2 networks," in *Proc. IEEE BMSB*, Nara, Japan, Jun. 2016, pp. 1–4.

[9] G. Martínez-Pinzón, N. Cardona, C. Garcia-Pardo, A. Fornés-Leal, and J. A. Ribadeneira-Ramírez, "Spectrum sharing for LTE-A and DTT: Field trials of an indoor LTE-A femtocell in DVB-T2 service area," *IEEE Trans. Broadcast.*, vol. 62, no. 3, pp. 552–561, Sep. 2016.

[10] L. Polak, O. Kaller, L. Klozar, and J. Prokopec, "Exploring and measuring the co-existence between LTE and DVB-T2-Lite services," in *Proc. Intl. Conf. Telecommun. and Sig. Process. (TSP)*, Rome, Italy, Jul. 2013, pp. 316–320.

[11] H. Bawab, P. Mary, J. F. Hélard, Y. Nasser, and O. Bazzi, "Spectral overlap optimization for DVB-T2 and LTE coexistence," *IEEE Trans. Broadcast.*, vol. 64, no. 1, pp. 70–84, Mar. 2018.

[12] A. J. Coulson, "Bit error rate performance of OFDM in narrowband interference with excision filtering," *IEEE Trans. Wireless Commun.*, vol. 5, no. 9, pp. 2484–2492, Sep. 2006.

[13] H. Wang, X. Zhang, and S. Wang, "Narrowband interference suppression in OFDM systems," in *Proc. Intl.l Conf. Wireless Commun. Sig. Process. (WCSP)*, Yangzhou, China, Oct. 2016, pp. 1–6.

[14] T. Weiss, J. Hillenbrand, A. Krohn, and F. K. Jondral, "Mutual interference in OFDM-based spectrum pooling systems," in *Prof. IEEE VTC-Spring*, Milan, Italy, May 2004, pp. 1873–1877.

[15] Q. Bodinier, F. Bader, and J. Palicot, "Coexistence in 5G: Analysis of cross-interference between OFDM/OQAM and legacy users," in *Proc. IEEE Globecom Wksp.*, Washington, DC, USA, Dec. 2016, pp. 1–6.

[16] P. Dharmawansa, N. Rajatheva, and H. Minn, "An exact error probability analysis of OFDM systems with frequency offset," *IEEE Trans. Commun.*, vol. 57, no. 1, pp. 26–31, Jan. 2009.

[17] J. Lee, H. l. Lou, D. Toumpakaris, and J. M. Cioffi, "SNR analysis of OFDM systems in the presence of carrier frequency offset for fading channels," *IEEE Trans. Wireless Commun.*, vol. 5, no. 12, pp. 3360–3364, Dec. 2006.

[18] K. A. Hamdi, "Exact SINR analysis of wireless OFDM in the presence of carrier frequency offset," *IEEE Trans. Wireless Commun.*, vol. 9, no. 3, pp. 975–979, Mar. 2010.

[19] Y. Medjahdi, M. Terré, D. L. Ruyet, and D. Roviras, "Interference tables: a useful model for interference analysis in asynchronous multicarrier transmission," *EURASIP J. Adv. Sig. Process.*, vol. 2014, no. 1, p. 54, Apr. 2014.

[20] O. Popescu and D. C. Popescu, "On the performance of sub-band precoded OFDM in the presence of narrowband co-channel interference," *IEEE Trans. Broadcast.*, vol. 62, no. 3, pp. 736–743, Sep. 2016.